


Discovery of a Selective 6-Hydroxy-1, 4-Diazepan-2-one Containing Butyrylcholinesterase Inhibitor by Virtual Screening and MM-GBSA Rescoring

Dose-Response:
An International Journal
April-June 2020:1-8
© The Author(s) 2020
Article reuse guidelines:
sagepub.com/journals-permissions
DOI: 10.1177/1559325820938526
journals.sagepub.com/home/dos



You Zhou¹ , Yanyu Hu², Xin Lu², Hongyu Yang², Qihang Li², Chenxi Du², Yao Chen³, Kwon Ho Hong⁴, and Haopeng Sun²

Abstract

Alzheimer disease (AD) is the most common form of dementia characterized by the loss of cognitive abilities through the death of central neuronal cells. In this study, structure-based virtual screens of 2 central nervous system-targeted libraries followed by molecular mechanics/generalized born surface area rescoring were performed to discover novel, selective butyrylcholinesterase (BChE) inhibitors, which are one of the most effective therapeutic strategies for the treatments in late-stage AD. Satisfyingly, compound 5 was identified as a highly selective low micromolar inhibitor of BChE (BChE IC₅₀ = 1.4 μM). The binding mode prediction and kinetic analysis were performed to obtain detailed information about compound 5. Besides, a preliminary structure–activity relationship investigation of compound 5 was carried out for further development of the series. The present results provided a valuable chemical template with a novel scaffold for the development of selective BChE inhibitors.

Keywords

Alzheimer disease, selective butyrylcholinesterase inhibitors, structure-based virtual screening, MM-GBSA rescoring, preliminary structure–activity relationship study

Introduction

Alzheimer disease (AD) is the most common form of dementia that causes problems with memory, thinking, and behavior. According to the World Alzheimer Report 2018,¹ there are currently about 30 million people having AD worldwide. The numbers of patients with AD are expected to increase 3-fold by 2050.¹ Alzheimer disease has become the third leading cause of death for the elderly, only after cardiovascular and cerebrovascular diseases and malignant tumors.²

Although the detailed pathogenesis of AD still remains unclear, several important clinical hallmarks, such as extracellular deposits of amyloid β (Aβ) peptides as senile plaques, intraneuronal neurofibrillary tangles, and large-scale neuronal loss are implicated in the occurrence and development of AD.³ Many hypotheses on the etiology of AD have been developed and tested, involving Aβ, Tau, cholinergic neuron damage and oxidative stress, and inflammation.^{4–7} However, therapies based on Aβ cascade hypothesis and/or tau hypothesis have been examined in clinical trials without promising results.⁸ Over the past decade, 3 cholinesterase inhibitors namely:

donepezil⁹, rivastigmine,¹⁰ and galantamine¹¹ have been approved by the FDA to treat patients with mild to moderately severe AD based on the cholinergic hypothesis,¹² according to which AD is accompanied by degeneration in cholinergic neurotransmission of the central nervous system (CNS). In the cholinergic hypothesis, the degeneration of cholinergic neurons

¹ College of Biotechnology, Southwest University, Chongqing, China

² School of Pharmacy, China Pharmaceutical University, Nanjing, China

³ School of Pharmacy, Nanjing University of Chinese Medicine, Nanjing, China

⁴ Department of Medicinal Chemistry, College of Pharmacy, University of Minnesota, Minneapolis, MN, USA

Received 23 April 2020; received revised 22 May 2020; accepted 27 May 2020

Corresponding Authors:

You Zhou, College of Biotechnology, Southwest University, Tiansheng Road#2, Chongqing 400715, China.

Email: zhouy701005@swu.edu.cn

Haopeng Sun, School of Pharmacy, China Pharmaceutical University, Nanjing 210009, China.

Email: sunhaopeng@163.com



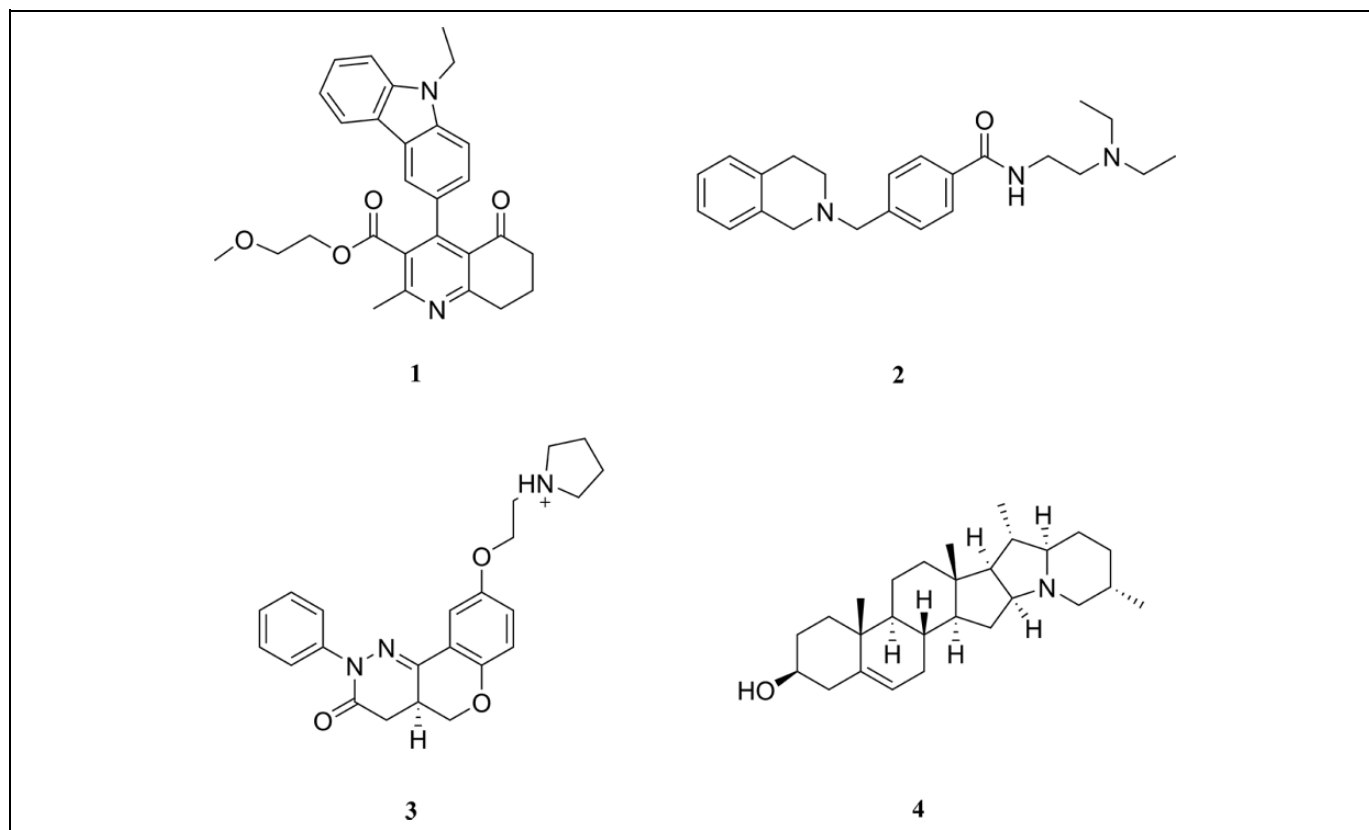


Figure 1. Chemical structures of recently reported BChE inhibitors identified via structure-based virtual screening.

and a deficiency of an important neurotransmitter acetylcholine (ACh) are correlated with the cognitive impairment in AD, and an increased level of ACh in the brain was supposed to be beneficial in AD treatment. There are 2 types of enzymes responsible for cholinergic transmission by hydrolyzing ACh within the human brain, namely acetylcholinesterase (AChE, EC 3.1.1.7) and butyrylcholinesterase (BChE, EC 3.1.1.8). Both enzymes share 50% identical amino acid sequence. The active site of both enzymes consists of a catalytic triad, an acyl-binding pocket, and a choline-binding site. Notably, smaller residues in the acyl-binding pocket of BChE provides a wider space. Although AChE plays the major role in the hydrolysis of ACh in the healthy brain, increasing experimental evidence has demonstrated that BChE takes over the hydrolysis of ACh in brains of patients with progressive AD. In progressed AD, the AChE level in the brain decreases from 55% to 67% of normal values, whereas BChE remains the same or increases up to 165% of the normal levels.^{13,14} Moreover, AChE knockout mice models indicated that BChE can potentially compensate the function of AChE, maintaining normal cholinergic pathways in AChE nullizygous animals.¹⁵ Several lines of evidence also indicated that BChE is implicated with A β aggregation during the senile plaque formation.¹⁶ In addition, BChE inhibition is not accompanied by the peripheral adverse effects, which hinder the clinical use of traditional AChE inhibitors.¹⁶ Taken together, the development of potent and selective BChE inhibitors with much reduced peripheral side

effects could be valuable for the treatment of patients with advanced AD.

Although many selective BChE inhibitors with diverse scaffolds, such as sulfonamide compounds, carbamate-based compounds, tacrine-based compounds, 3,4,5,6-tetrahydroazepino [4, 3-*b*]indol-1(6H)-one (THAI) compounds have been reported, none of them successfully entered into clinical as anti-AD drugs.¹⁵ Thus, more efforts should be devoted to the discovery and development of potent inhibitors targeting BChE. Over the past decade, multiple X-ray crystallographic structures of BChE proteins in complex with highly potent and selective human BChE inhibitors have been reported,¹⁷⁻²¹ which sets the stage for structure-based virtual screening. So far, there are few report of using the structure-based virtual screening protocol to discover potent and selective BChE inhibitors (Figure 1).^{13,22} In 2016, Ross et al screened a combination of 2 libraries by using a structure-based virtual screening approach and identified compound 1 with potent and selective BChE inhibitory activity (equine BChE IC_{50} = 9.72 μ M; *Electrophorus electricus* AChE = 1.35% at 10 μ M). The follow-up structure-activity relationship (SAR) study resulted in active compounds which possessed highly selective BChE inhibitory activity and predicted high blood-brain barrier (BBB) permeability.¹³ In 2019, Zhang et al reported compound 2 (BChE IC_{50} = 17.94 μ M; AChE IC_{50} > 50 μ M) by performing structure-based virtual screening of in-house compound library and in vitro BChE/AChE assay. The subsequent molecular

docking-guided chemical optimization and SAR study based on hit 2 generated some new potent selective BChE inhibitors with anti-A β aggregation activity.²² In addition, compounds 3 (equine BChE IC₅₀ = 8.3 μ M) and 4 (BChE IC₅₀ = 16.8 nM; AChE = 10% at 5 μ M) were identified as new BChE inhibitors via structure-based virtual screening by Atatreh et al²³ and Zhan et al²⁴ respectively.

In this work, structure-based virtual screens of 2 CNS-targeted libraries followed by molecular mechanics/generalized born surface area (MM-GBSA) rescoring were performed to discover novel, selective BChE inhibitors. Eight potential hits were purchased for in vitro testing using modified Ellman method. The kinetic analysis and binding mode study were performed to obtain detailed information about active hit compounds. In addition, a preliminary SAR study was conducted, and the result was supposed to be beneficial for further extensive SAR study.

Materials and Methods

Molecular Modeling

Protein and ligand library preparation. Compounds from 2 CNS-targeted databases (Enamine CNS Library and ChemDiv CNS-MPO Library) were subjected to the LigPrep module of the Schrödinger molecular modeling suite 2017 (Schrödinger, Inc, LLC) to generate 3D structures including all possible stereoisomers and tautomers.²⁵

The crystallographic structure of human BChE was downloaded from Protein Data Bank (<http://www.rcsb.org>, PDB: 5NN0).²⁰ All solvent molecules except HOH724, HOH734, and HOH805 were eliminated. The raw PDB protein structure was then prepared by giving preliminary treatment including adding hydrogen atoms, refining the loop region, and finally energy minimization by using the Protein Preparation Wizard of the Schrödinger modeling suite.²⁶

Virtual screening. The generated 3D structures were subjected to a hierarchical docking-based virtual screening workflow using the docking module of the Schrödinger suite, Glide (Grid-based ligand docking with energetics).²⁵ At the beginning, the prepared libraries were screened using glide high-throughput virtual screening mode. Compounds with better performance (Docking score ≤ -7) were screened using standard precision (SP) docking mode. Next, potential hit compounds (Docking score ≤ -8) from SP docking were processed through extra-precision (XP) docking mode. The output of XP docking was filtered for an XP Gscore of ≤ -9 .

MM-GBSA rescoring. The MM-GBSA method is widely exploited to investigate the binding of small ligands to the macromolecules and rank affinities of ligands bound to the same macromolecule.²⁷ The binding free energies of the filtered output of XP docking were estimated by using the Prime MM-GBSA Panel of the Schrödinger modeling suite. Distance from ligand was set to 5 Å. Other parameters were maintained as the defaults. The threshold for the binding free

energy (dG) was set to a value of -90 kcal/mol. Finally, 9 hits were identified and 8 available hits were purchased from Topscience (www.tsbiochem.com), with purity $>95\%$ (liquid chromatography-mass spectrometry).

Biological Assessment

In vitro cholinesterase inhibition assay. The cholinesterase inhibitory activity of all compounds was determined by a modified Ellman assay.²⁸⁻³⁰ AChE (from human erythrocytes, C0663), BChE (from human serum, B4186), 5,5-dithiobis-(2-nitrobenzoic acid; DTNB, D218200), acetylthiocholine iodide (ATC, A5751), and butyrylthiocholine iodide (BTC, B3253) were purchased from Sigma-Aldrich.

For measurement, a cuvette containing 40 μ L of phosphate buffer pH 8.0, 10 μ L of AChE (2.5 units/mL) or BChE (2.5 units/mL), and 10 μ L of the test compound solution was allowed to stand for 5 minutes before 20 μ L of DTNB (0.01 M) was added. After the addition of 20 μ L of ATC (0.075 M) or BTC (0.075 M), the reaction was initiated and the solution was mixed immediately. Two minutes after substrate addition, the absorption was measured at 412 nm by Thermo Fisher Scientific spectrophotometer (Multiskan FC). Ten microliters of phosphate-buffered solution replaced the enzyme solution were used to determine the blank value. The percentage of inhibition (I) was calculated according to the formula: $I = (Ac - Ai)/(Ac - Ab) \times 100\%$, with Ai, Ac, and Ab representing the change in the absorbance in the presence of an inhibitor, without an inhibitor and without enzyme, respectively. To determine IC₅₀ values, a dilution series of 6 different concentrations (10^{-4} to 10^{-9} M) were prepared for each compound. The inhibition curve was drawn by plotting the percentage enzyme activity (100% for the reference) versus the logarithm of the test compound concentration using GraphPad Prism 6 (GraphPad Software).

Kinetic study. Kinetic study of BChE inhibition was performed as described in Section 2.2.1. Briefly, the substrate (BTC) was used at various concentrations (90, 150, 226, 452, and 904 μ M) for each test compound concentration and the enzymatic reaction was extended to 4 minutes before determining the absorption. The V_{max} and K_m values of the Michaelis–Menten kinetics were calculated by nonlinear regression from substrate–velocity curves using GraphPad Prism 6 (GraphPad Software). Inhibition constants were evaluated from the effect of substrate concentration (S) on the degree of inhibition according to the following equation:

$$V_0 = V_{max}[S]/\left(K_m(1 + [I]/K_{ic}) + [S](1 + [I]/K_{iu})\right),$$

where S is the substrate BTC, I is the inhibitor, K_{ic} is the enzyme–inhibitor inhibition constant of a complex formed at the catalytic site, K_{iu} is the Michaelis complex–inhibitor inhibition constant of a complex formed at the peripheral site, K_m is the Michaelis constant, and V_m is maximal velocity.

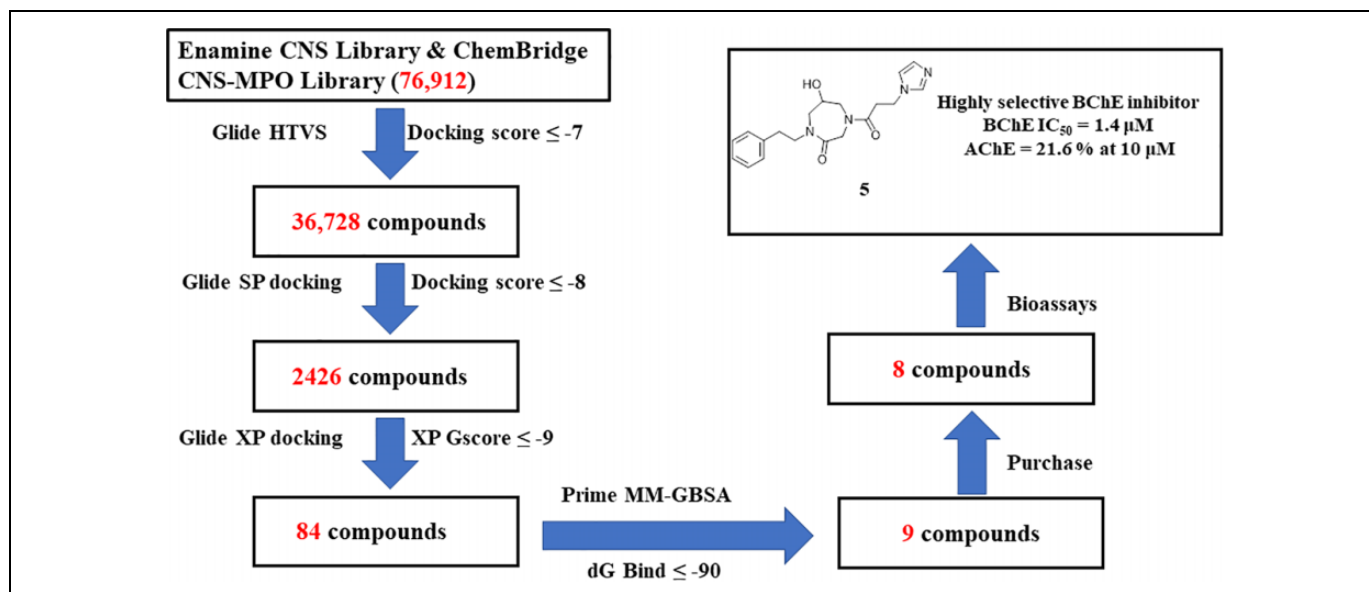


Figure 2. Docking-based virtual screening protocol used in the virtual screening workflow. A 3-step molecular docking protocol comprised of high-throughput virtual screening (HTVS), standard precision (SP) docking, and extra-precision (XP) docking.

Results and Discussion

Drug discovery within CNS area has specific and unique demands for physicochemical and structural properties of compounds: Compounds must permeate the BBB; should be less polar, smaller, and more rigid than non-CNS molecules; and have strong constraints on the number and/or type of functional groups.³¹ Central nervous system multiparameter optimization (MPO) score is now a well-recognized algorithm in the CNS-focused medicinal chemistry community.³² In our study, we performed virtual screens of 2 CNS-targeted libraries, Enamine CNS Library (47 040 compounds) and ChemDiv CNS-MPO Library (29 872 compounds), which are specifically designed for CNS drug discovery via MPO for improved BBB permeability. The crystallographic structure of BChE in complex with *N*-((1-(2,3-dihydro-1*H*-inden-2-yl)piperidin-3-yl)methyl)-*N*-(2-(dimethylamino)ethyl)-2-naphthamide (PDB ID: 5NN0)²⁰ was used in the structured-based virtual screening. Briefly, a 3-step molecular docking protocol was performed using the Glide module of the Schrödinger suite to narrow down the number of screening compounds by gradually increase docking precisions (Figure 2). After docking, 84 compounds were retained and subjected to the subsequent binding free energy calculations using MM-GBSA method. The threshold for the binding free energy (dG) was set to a value of -90 kcal/mol. Nine compounds with lower dG bind values than this threshold were identified. Finally, 8 commercial available compounds were purchased for experimental validation (Figure 3). Result demonstrated that none of the compounds showed significant inhibition against AChE at 10 μ M (Table S1). Among them, only 4-(3-(1*H*-imidazol-1-yl)propanoyl)-6-hydroxy-1-phenethyl-1,4-diazepan-2-one (5) showed moderate inhibition of BChE (BChE = 66% at 10 μ M). Next, the dose-dependent inhibitory activities of compound 5 against BChE

were tested at doses ranging from 10^{-4} to 10^{-9} M. The result demonstrated that compound 5 showed great anti-BChE activity ($IC_{50} = 1.4$ μ M; Figure S1). A literature survey indicated that compound 5 was structurally different from the previously reported BChE inhibitors and can act as a starting point for further studies to develop new BChE inhibitors as anti-AD agents.

To gain information on the mechanism of inhibition, compound 5 was selected to perform enzymatic kinetic studies with BChE. As shown in Figure 4 and Table S2, the pattern clearly demonstrates that compound 5 is a mixed-type inhibitor: the presence of 5 reduces the maximum velocity V_m and increases the K_m value. It means that compound 5 can bind to both the free enzyme and the enzyme-substrate complex.³³ The inhibition constant K_i values of 5 for the competitive part and the uncompetitive part of inhibition are 0.54 ± 0.07 μ M and 2.9 ± 1.0 μ M, respectively.

The prediction of a potential binding mode of compound 5 to the catalytic active site (CAS) of BChE was performed to obtain more detailed information (Figure 5). The docking conformation suggested that compound 5 occupied the CAS adopting a U-shaped conformation, which is common to potent BChE inhibitors.^{19,28} In detail, the imidazole ring formed strong π - π interactions and a cation- π interaction with TRP82 in the choline-binding pocket and formed a salt bridge with GLU197 located at the bottom of CAS. The 6-hydroxy group on the 1,4-diazepan-2-one ring contacted with ALA328 in the choline-binding pocket through H-bonding interaction. Additionally, 2-carbonyl group of 1,4-diazepan-2-one ring formed a water-mediated H-bond with THR120. The phenyl group occupied the acyl-binding pocket and interacted with TRP231 via π - π interactions (T-stacking). Since the interactions with TRP82 and TRP231 were considered important in BChE inhibition, the role of the 2 key fragments (imidazole and benzene)

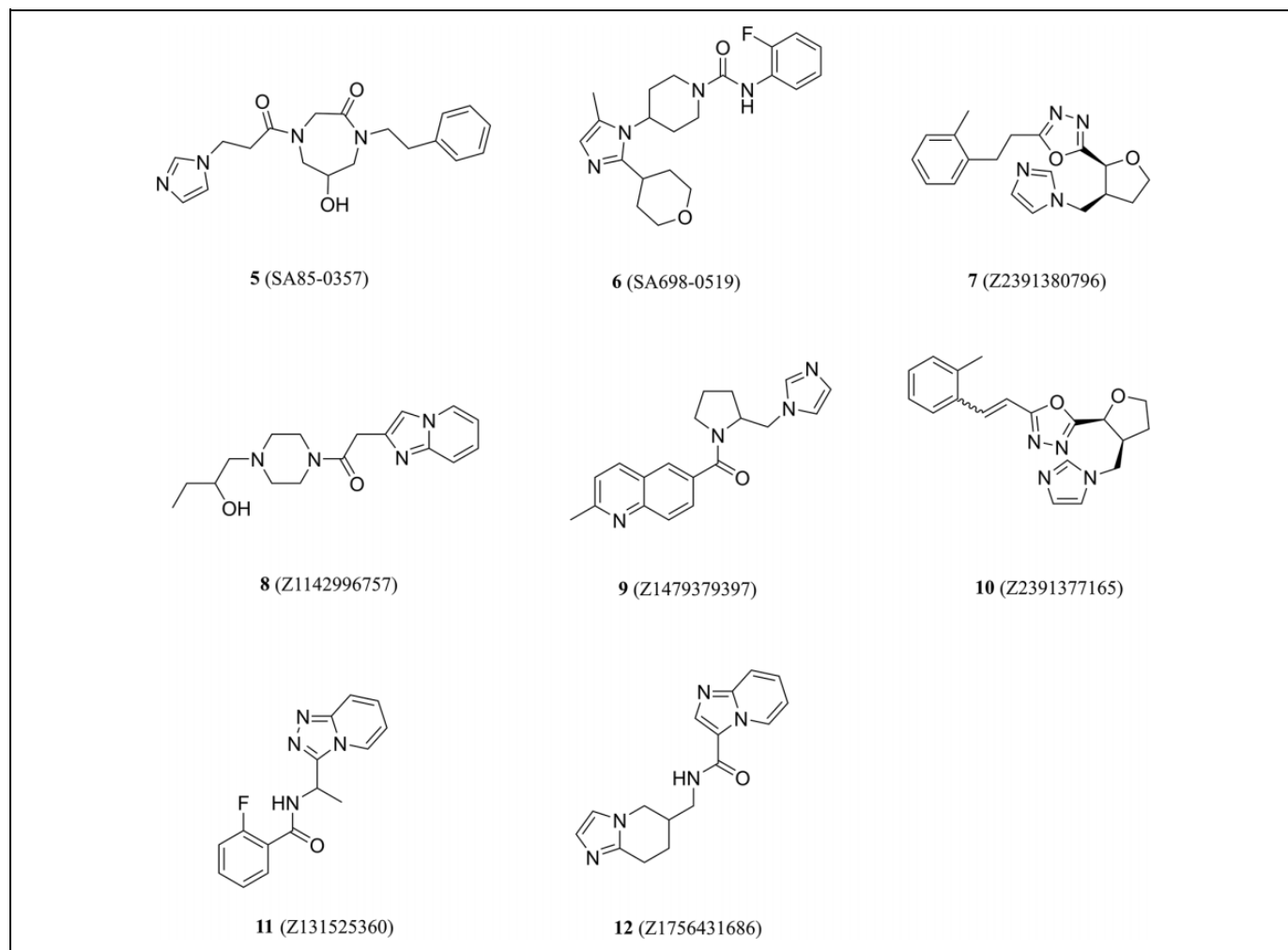


Figure 3. Chemical structures of the compounds purchased for in vitro tests.

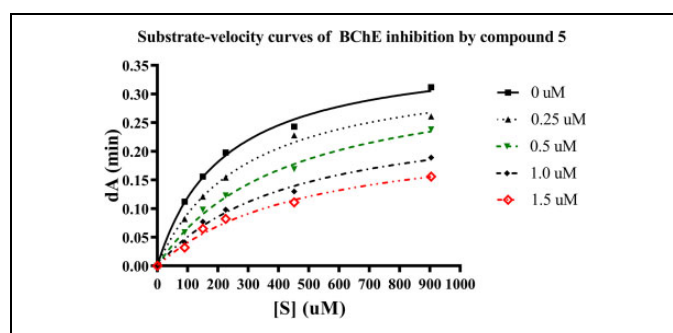


Figure 4. Representative plot of BChE activity and the effect of substrate concentration (90-904 μM) in the absence of inhibitor and in the presence of 5 (0.25-1.5 μM).

should be assessed before performing further chemical modifications.

To preliminarily elucidate the SAR of hit compound 5, a similarity search was performed by using 5 as the template molecule and screening the ChemDiv database (<http://chemistrondemand.com>). Based on the searching results (similarity

= 0.4, 1146 compounds), 4 analogs of 5 were purchased from Topscience (www.tsbiochem.com) and subjected to in vitro enzyme inhibition assay (Figure 6). Result showed that none of them had potent inhibitory activity against cholinesterase proteins at the concentration of 50 μM (Figure S2). The preliminary SAR was summarized in Figure 7: (1) decreasing the amide chain length (compound 13) led to a significant change in the activity, suggesting that the chain length plays an important role in its activity. We speculated that the interaction strength between imidazole group of 13 and amino acid residues (TRP82 and GLU197) might be weakened; and (2) replacing imidazole group with phenyl group (compound 14) and cyclopentane group (compound 15) also resulted in a large decrease in the activity, which further emphasized the important role of imidazole group in ligand binding. In addition, the protonated imidazole group might contribute to the initial molecular recognition between compound 5 and ASP70 in the peripheral binding site of BChE³⁴; (3) the activity loss was observed when the phenyl group replaced with isopropyl groups (compound 16). It might be related with the loss of T- π stacking interactions between 5 and surrounding TRP231.

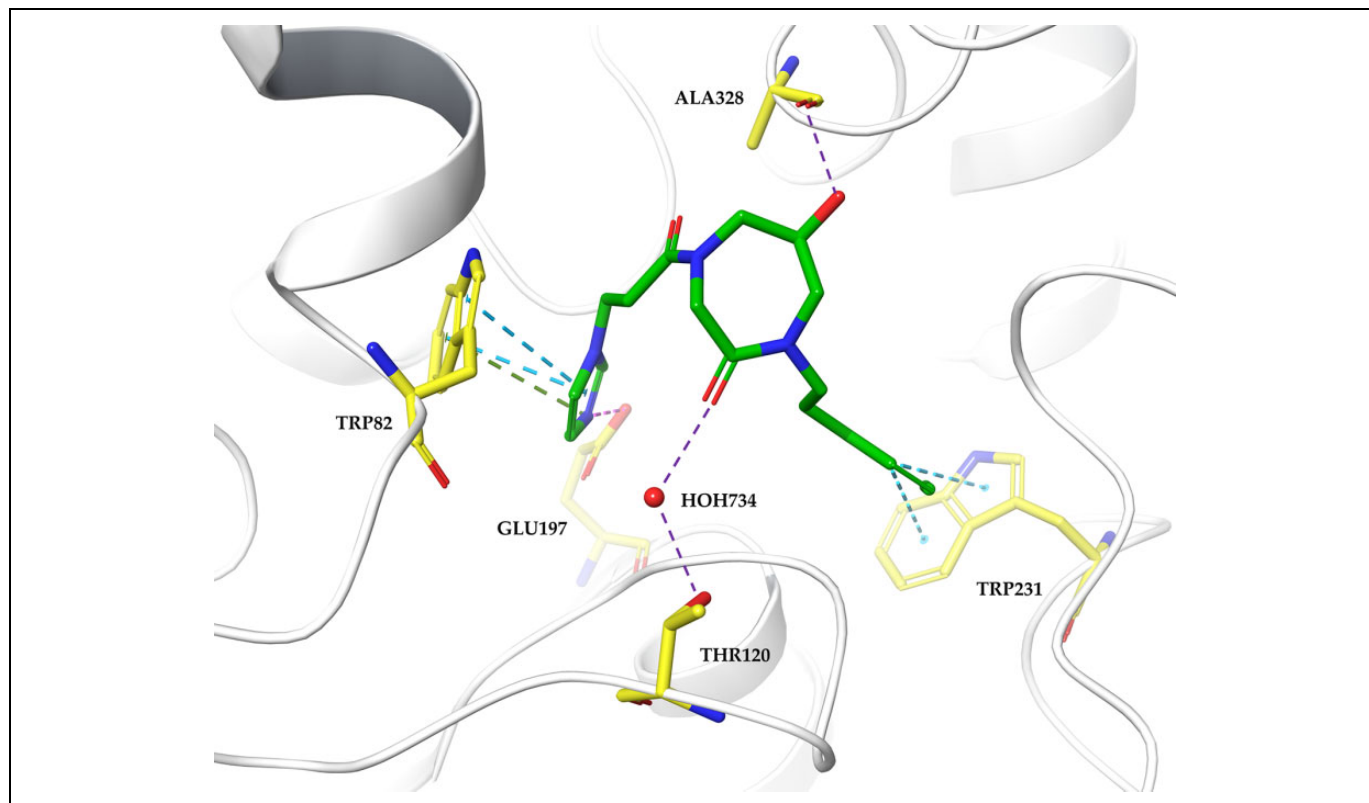


Figure 5. Binding mode predictions for compound 5 with BChE domain (PDB ID: 5NN0). Compound 5 was shown in green stick mode; key residues were shown in yellow stick mode. The purple dashed line represents a hydrogen bond, the green dashed lines represent cation- π stackings, the magenta dashed lines represent an ionic interaction, and the light blue dashed lines represent π - π stackings.

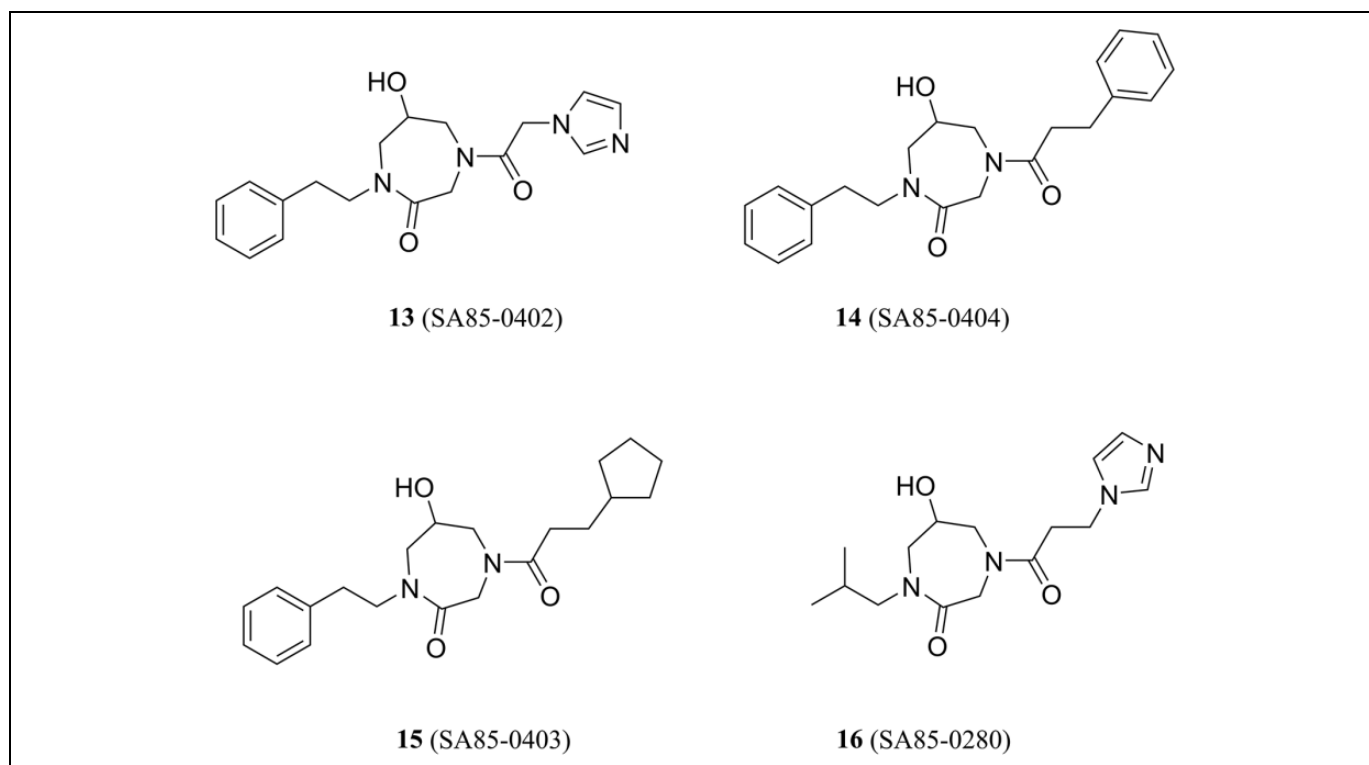


Figure 6. Chemical structures of hit compound 5 analogues.

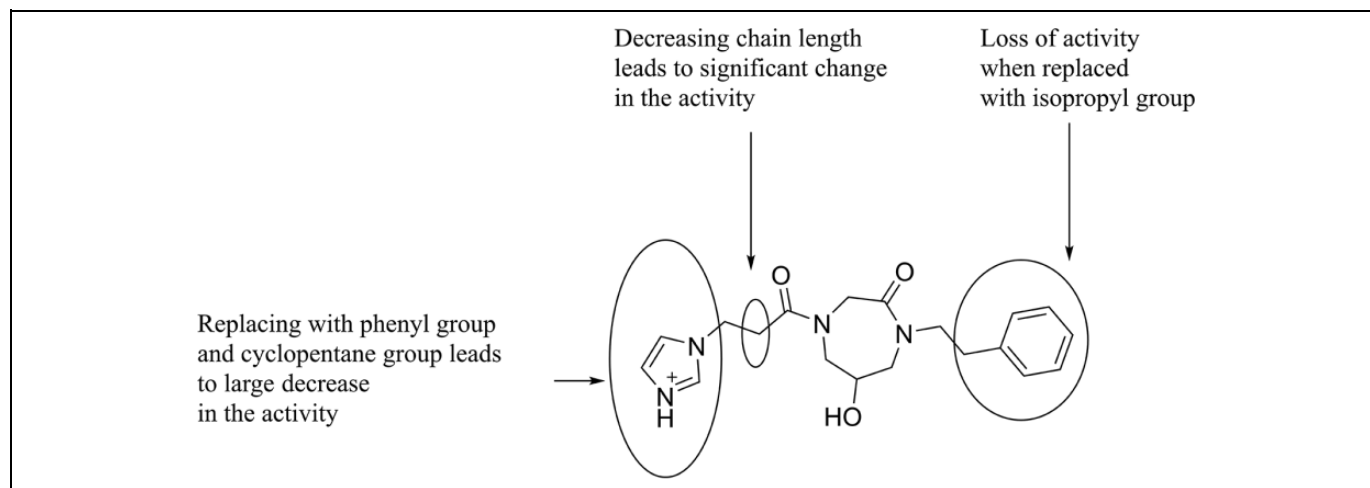


Figure 7. Preliminary SARs of the BChE inhibitor class based on 5.

Based on our binding mode analysis and the preliminary SAR study result, further SAR study based on hit compound 5 is processing.

Conclusion

In this study, we applied the Schrödinger docking-based virtual screening workflow, followed by an MM-GBSA rescoring step, to discover potent and selective BChE inhibitors with predicted high BBB permeability. Using this protocol, we narrowed down 76 912 molecules from 2 CNS-targeted libraries to 9 molecules, and 8 commercial available molecules were purchased and evaluated in vitro for cholinesterase inhibition. According to in vitro enzyme inhibition tests, compound 5 containing 6-hydroxy-1,4-diazepan-2-one scaffold was first reported as a novel, selective BChE inhibitor (BChE IC_{50} = 1.4 μ M). In addition, the result of kinetic studies indicated a mixed-type inhibition of compound 5 toward BChE. Furthermore, docking studies and preliminary SAR studies were performed to obtain more detailed information about compound 5. Due to the preliminary results, 5 emerged as a promising molecule for further development for AD treatment.

Declaration of Conflicting Interests

The author(s) declared no potential conflicts of interest with respect to the research, authorship, and/or publication of this article.

Funding

The author(s) disclosed receipt of the following financial support for the research, authorship, and/or publication of this article: This work was supported by Fundamental Research Funds for the Central Universities under Grant No. XDJK2019C103; National Natural Science Foundation of China [grant numbers 81803367, 81872728, and 81573281]; Basic Research and Frontier Exploration Project of Chongqing [grant number cstc2018jcyjAX0715]; Natural Science Foundation of Jiangsu Province [grant number BK20191411]; Jiangsu Qinglan Project and Venture & Innovation Support Program for Chongqing Overseas Returnees.

ORCID iD

You Zhou  <https://orcid.org/0000-0002-4404-1491>

Supplemental Material

Supplemental material for this article is available online.

References

1. Alzheimer's Disease International. World Alzheimer Report 2018. The state of the art of dementia research: new frontiers. 2018. Accessed April 23, 2020. <https://www.alz.co.uk/research/world-report-2018>
2. Alzheimer's Disease International. World Alzheimer report 2015: the global impact of dementia. 2015. Accessed April 23, 2020. <https://www.alz.co.uk/research/world-report-2015>
3. Li H, Wang X, Yu H, et al. Combining in vitro and in silico approaches to find new candidate drugs targeting the pathological proteins related to the Alzheimer's disease. *Curr Neuropharmacol*. 2018;16(6):758-768.
4. Sanabria-Castro A, Alvarado-Echeverría I, Monge-Bonilla C. Molecular pathogenesis of Alzheimer's disease: an update. *Ann Neurosci*. 2017;24(1):46-54.
5. Jiang T, Sun Q, Chen S. Oxidative stress: a major pathogenesis and potential therapeutic target of antioxidative agents in Parkinson's disease and Alzheimer's disease. *Prog Neurobiol*. 2016;147:1-19.
6. Zott B, Simon MM, Hong W, et al. A vicious cycle of β amyloid-dependent neuronal hyperactivation. *Science*. 2019;365(6453):559-565.
7. Du X, Wang X, Geng M. Alzheimer's disease hypothesis and related therapies. *Transl Neurodegener*. 2018;7(2):1-7.
8. Kodamullil AT, Zekri F, Sood M, et al. Tracing investment in drug development for Alzheimer disease. *Nat Rev Drug Discov*. 2017;16(12):819.
9. Prvulovic D, Schneider B. Pharmacokinetic and pharmacodynamic evaluation of donepezil for the treatment of Alzheimer's disease. *Expert Opin Drug Metab Toxicol*. 2014;10(7):1039-1050.

10. Birks JS, Grimley Evans J. Rivastigmine for Alzheimer's disease. *Cochrane Database Syst Rev*. 2015;10(4):Cd001191.
11. Prvulovic D, Hampel H, Pantel J. Galantamine for Alzheimer's disease. *Expert Opin Drug Metab Toxicol*. 2010;6(3):345-354.
12. Contestabile A. The history of the cholinergic hypothesis. *Behav Brain Res*. 2011; 221(2):334-340.
13. Dighe SN, Deora GS, Mora ED, et al. Discovery and structure-activity relationships of a highly selective butyrylcholinesterase inhibitor by structure-based virtual screening. *J Med Chem*. 2016; 59(16):7683-7689.
14. Arendt T, Bigl V, Walther F, Sonntag M. Decreased ratio of CSF acetylcholinesterase to butyrylcholinesterase activity in Alzheimer's disease. *Lancet*. 1984;1(8369):173.
15. Li Q, Yang HY, Chen Y, Sun HP. Recent progress in the identification of selective butyrylcholinesterase inhibitors for Alzheimer's disease. *Eur J Med Chem*. 2017;132(26):294-309.
16. Greig NH, Utsuki T, Ingram DK, et al. Selective butyrylcholinesterase inhibition elevates brain acetylcholine, augments learning and lowers Alzheimer β -amyloid peptide in rodent. *Proc Natl Acad Sci USA*. 2005;102(47):17213-17218.
17. Brus B, Kořak U, Turk S, et al. Discovery, biological evaluation, and crystal structure of a novel nanomolar selective butyrylcholinesterase inhibitor. *J Med Chem*. 2014;57(19):8167-8179.
18. Šink R, Brazzolotto X, Knez D, et al. Structure-based development of nitroxoline derivatives as potential multifunctional anti-Alzheimer agents. *Bioorg Med Chem*. 2015;23(15):4442-4452.
19. Kořak U, Brus B, Knez D, et al. Development of an in-vivo active reversible butyrylcholinesterase inhibitor. *Sci Rep*. 2016;6: 39495-39519.
20. Kořak U, Brus B, Knez D, et al. The magic of crystal structure-based inhibitor optimization: development of a butyrylcholinesterase inhibitor with picomolar affinity and in vivo activity. *J Med Chem*. 2018;61(1):119-139.
21. Meden A, Knez D, Jukić M, et al. Tryptophan-derived butyrylcholinesterase inhibitors as promising leads against Alzheimer's disease. *Chem Commun*. 2019;55(26):3765-3768.
22. Jiang CS, Ge YX, Cheng ZQ, et al. Discovery of new selective butyrylcholinesterase (BChE) inhibitors with anti-A β aggregation activity: structure-based virtual screening, hit optimization and biological evaluation. *Molecules*. 2019;24(14):2568-2588.
23. Atatreh N, Rawashdah SA, Neyadi SSA, Sawsan MA, Mohammad AG. Discovery of new butyrylcholinesterase inhibitors via structure-based virtual screening. *J Enzyme Inhib Med Chem*. 2019;34(1):1373-1379.
24. Zhou S, Yuan Y, Zheng F, Zhan C. Structure-based virtual screening leading to discovery of highly selective butyrylcholinesterase inhibitors with solanaceous alkaloid scaffolds. *Chem Biol Interact*. 2019;308:372-376.
25. Friesner RA, Banks JL, Murphy RB, et al. Glide: a new approach for rapid, accurate docking and scoring. 1. Method and assessment of docking accuracy. *J Med Chem*. 2004;47(7):1739-1749.
26. Sastry GM, Adzhigirey M, Day T, Ramakrishna A, Woody S. Protein and ligand preparation: parameters, protocols, and influence on virtual screening enrichments. *J Comput Aided Mol Des*. 2013;27(3):221-234.
27. Genheden S, Ryde U. The MM/PBSA and MM/GBSA methods to estimate ligand-binding affinities. *Expert Opin Drug Discov*. 2015;10(5):449-461.
28. Zhou Y, Lu X, Yang H, et al. Discovery of selective butyrylcholinesterase (BChE) inhibitors through a combination of computational studies and biological evaluations. *Molecules*. 2019;24(23): 4217-4231.
29. Yang Z, Shi J, Xie J, et al. Large-scale generation of functional mRNA-encapsulating exosomes via cellular nanoporation. *Nat Biomed Eng*. 2020;4(1):69-83.
30. Ellman GL, Courtney KD, Andres V Jr, Featherstone RM. A new and rapid colorimetric determination of acetylcholinesterase activity. *Biochem Pharmacol*. 1961;7(2):88-95.
31. Mayol-Llinàs J, Nelson A, Farnaby W, Ayscough A. Assessing molecular scaffolds for CNS drug discovery. *Drug Discovery Today*. 2017;22(7):965-969.
32. Wager TT, Hou X, Verhoest PR, Villalobos A. Central nervous system multiparameter optimization desirability: application in drug discovery. *ACS Chem Neurosci*. 2016;7(6):767-775.
33. Šinko G, Brglez J, Kovarik Z. Interactions of pyridinium oximes with acetylcholinesterase. *Chem Biol Interact*. 2010;187(1-3): 172-176.
34. Masson P, Froment MT, Bartels CF, Lockridge O. Asp70 in the peripheral anionic site of human butyrylcholinesterase. *Eur J Biochem*. 1996;235(1-2):36-48.